Acta Geologica Sinica (English Edition), 2019, 93(1): 244–245

Research Advances

The Carbon Isotope Fluctuations across the Lower–Middle Jurassic Boundary and the Paleoclimate Changes

YI Haisheng[1, *], XIA Guoqing[1], LI Gaojie[1], YI Fan[2], ZHANG Shuai[2], CAI Zhanhu[2], JIAO Haijing[3] and WU Chihua[3]

[1] *Institute of Sedimentary Geology, Chengdu University of Technology, Chengdu 610059, China*
[2] *College of Earth Sciences, Chengdu University of Technology, Chengdu 610059, China*
[3] *School of Marine Sciences, Sun Yat-sen University, Guangzhou 510006, China*

Citation: Yi et al., 2019. The Carbon Isotope Fluctuations across the Lower–Middle Jurassic Boundary and the Paleoclimate Changes. *Acta Geologica Sinica* (English Edition), 93(1): 244–245. DOI: 10.1111/1755-6724.13660

Objective

The Qiangtang Basin of Tibetan Plateau most widely outcrops marine Jurassic strata in China, even in eastern Asian, and the Jurassic strata and ammonites' occurrence are in favor of researching evolution of paleoceanography in the Tethyan region and global stratigraphic comparison. This work focused on the carbon isotope changes across the J_1–J_2 boundary in the eastern Tethys region.

Methods

Exiubu section located at the Amdo area of Qiangtang Basin, where the Lower Jurassic Quse Formation and Middle Jurassic Sewa Formation deposited continuously with late Toarcian to Aalenian ammonites at the J_1–J_2 boundary (Yin Jiarun et al., 2006). We collected 60 samples with a mean spacing of 2 m at the boundary, and these samples are black shales, calcareous mudstones, marls and micrites. One hundred and twenty carbonates samples have been carried out for carbon and oxygen isotopes of carbonate contents, and sixty samples for organic carbon contents and isotopes. Fig. 1 is the carbon isotopes and climate changes curves at the J_1–J_2 boundary of Exiubu section, Amdo area of Tibet. To visually express the change process of the analysis data, the original data is smoothed by Moving Median (Appendix 1).

According to the simultaneous analysis of 60 samples of organic carbon ($\delta^{13}C_{ORG}$) and inorganic carbon ($\delta^{13}C_{CAL}$) results, the $\delta^{13}C_{ORG}$ varies between −22.3‰ and −25.3‰ (PDB) with an average value of −24.05‰ (PDB), and the $\delta^{13}C_{CAL}$ varies from 2.1‰ to −5.3‰ with an average value of −1.12‰ (Fig. 1), which shows the positive excursions observed in the $\delta^{13}C_{ORG}$ records in the upper part (0–60 cm depth) of Quse Formation (Lower Jurassic) and the negative excursions in the Sewa Formation (60–120 m depth); especially at the J_1–J_2 boundary, the $\delta^{13}C_{ORG}$ values gradually decline and the Δ value is 3‰ (Δ=3‰). Furthermore, the change of the inorganic carbon $\delta^{13}C_{ORG}$ of in the J_1–J_2 profile boundary is similar to that of $\delta^{13}C_{CAL}$. The top of Quse Formation (Lower Jurassic) exhibits carbon-isotopic values much richer than Sewa Formation (Middle Jurassic), and at the 30–70 m depth, the $\delta^{13}C_{CAL}$ records reach the maximum positive carbon-isotope excursion of 1.8‰.

* Corresponding author. E-mail: yhs@cdut.edu.cn

Results

The carbon-isotopes of the modern terrigenous organic matters have an average value of −27‰, and the marine matters of −21‰. However, the carbon isotopes of the marine organic matters in ancient sea are changeable. For example, the Cambrian $\delta^{13}C_{ORG}$ records reach the minimum values of −36‰, and the Cretaceous ones have a value of −28‰. At present, the equation about the $\delta^{13}C$ and CO_2 concentration is mainly concerned with the fractional effect between the $\delta^{13}C_{POC}$ of marine particulate organic matter and CO_2 concentration of seawater. They were proposed by Fischer et al. (1998) and Bentaleb et al. (1998)

$$[CO_2] = (\delta^{13}C_{ORG}+14.95)/ (-0.53)$$

$$[CO_2] = (\delta^{13}C_{ORG}+14.38)/ (-0.59)$$

$$P_{CO2} = [CO_2]/K_0$$

Where $\delta^{13}C_{ORG}$ is value of the organic carbon isotopes with ‰ (PDB), and the CO_2 and P_{CO2} with μmole/kg and μatm, respectively. K_0 is the solubility constant, and salinity (S) is 35%. The K_0 value is 0.0398 when the temperature (T) in modern seawater is 15°C, and the calculated P_{CO2} shows the CO_2 pressure of sea surface.

According to the above-mentioned equations, the P_{CO2} concentrations at the J_1–J_2 boundary reach the minimum value of 375 μatm, and the maximum value of 485 μatm, which indicates they are about 195–305 higher than those in Quaternary when they are of 180 μatm at glaciation and 280 μatm at interglaciation. The seafloor sediments in modern sea and Quaternary show the $\delta^{13}C$ values of phytoplankton, grains and sediments are controlled by the dissoluble CO_2 compositions of seawater, and the fractionation equation is established. The CO_2 compositions calculated by this equation have a certain differentiation, but the inverse relationship between $\delta^{13}C$ and CO_2 concentration is common which provides a theoretical basis for reconstructing the paleo-atmospheric P_{CO2} concentrations. We define the relative values of P_{CO2} as ΔP_{CO2} which means the deviation between calculated P_{CO2} and an average value. The positive values of ΔP_{CO2} indicate greenhouse, and the negative values indicate

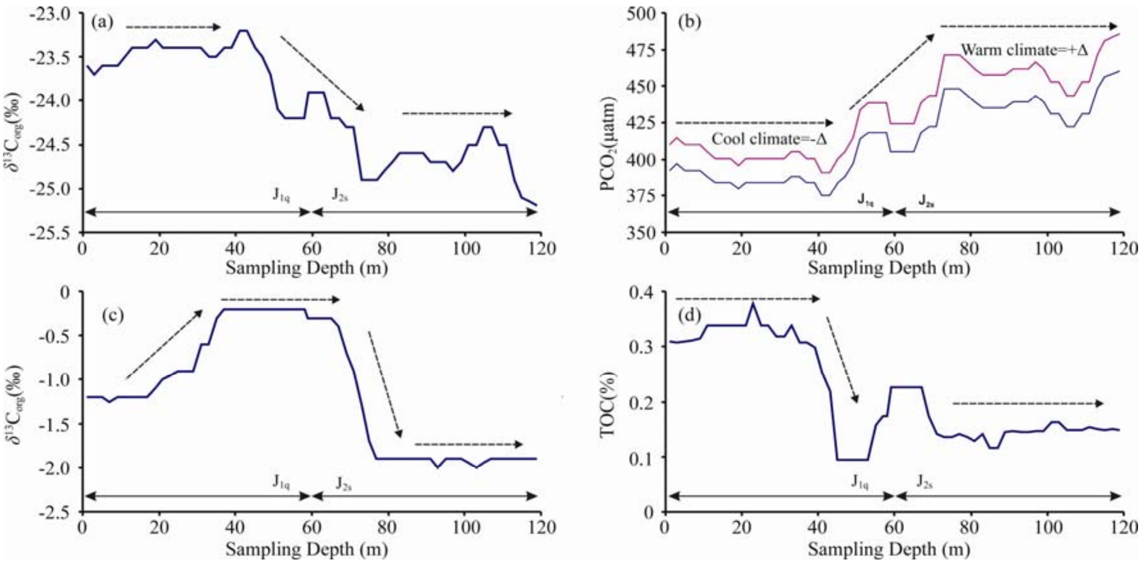

Fig. 1. The carbon isotopes and climate changes curves at the J_1–J_2 boundary of Exiubu section, Amdo area of Tibet.

icehouse. Consequently, the effect of diagenesis and land-mixing can be eliminated.

Conclusion

According to the paleo-P_{CO2} change in the section, the Quse Formation of Early Jurassic has low values, and the Sewa Formation of Middle Jurassic has high values. The climate of J_1–J_2 boundary changes from the relatively cool to warm period with the gradually rise of $P_{CO2.}$ The carbonate carbon isotopes synchronously occurs positive excursions at the J_1–J_2 boundary.

Acknowledgements

This work was supported by the National Natural Science Foundation of China (grants No. 41572089 and 41572095).

References

Bentaleb, I., and Fontugne, M., 1998. The role of the southern Indian Ocean in the glacial to interglacial atmospheric CO_2, change: organic carbon isotope evidences. *Global & Planetary Change*, 16–17(1): 25–36.

Fischer, G., Müller, P.J., and Wefer, G., 1998. Latitudinal ^{13}Corg variations in sinking matter and sediments from the South Atlantic: effects of anthropogenic CO_2 and implications for paleo-PCO_2 reconstructions. *Journal of Marine Systems*, 17(1–4): 471–495.

Yin Jiarun, Gao Jinhan, Wang Yongsheng, Zhan Shuqi , Zheng Chunzi, Xu Debiao, Bai Zhida, Sun Lixin and Su Xin, 2006. Jurassic ammonites in anoxic black shales from Sewa and Amdo, northern Tibet. *Acta Palaeontologica Sinica*, 45(3): 311–331 (in Chinese with English abstract).

Appendix 1 Carbon isotope values of carbonate and organic matter from the Exiubu section

Sampling Depth (m)	Sample label	$\delta^{13}C_{Carb}$ (‰, PDB)	$\delta^{13}C_{org}$ (‰, PDB)	Sampling Depth (m)	Sample label	$\delta^{13}C_{Carb}$ (‰, PDB)	$\delta^{13}C_{org}$ (‰, PDB)
1	EXPS-123	−1.2	−23.6	59	EXPq-03	−0.3	−23.9
3	EXPS-119	−1.2	−23.7	63	EXPq-07	−0.3	−23.9
5	EXPS-115	−1.2	−23.6	65	EXPq-11	−0.3	−24.2
7	EXPS-111	−1.3	−23.6	67	EXPq-15	−0.4	−24.2
9	EXPS-107	−1.2	−23.6	69	EXPq-19	−0.7	−24.3
11	EXPS-103	−1.2	−23.5	71	EXPq-23	−0.9	−24.3
13	EXPS-99	−1.2	−23.4	73	EXPq-27	−1.3	−24.9
15	EXPS-95	−1.2	−23.4	75	EXPq-31	−1.7	−24.9
17	EXPS-91	−1.2	−23.4	77	EXPq-35	−1.9	−24.9
19	EXPS-87	−1.1	−23.3	79	EXPq-39	−1.9	−24.8
21	EXPS-81	−1.0	−23.4	81	EXPq-43	−1.9	−24.7
23	EXPS-77	−1.0	−23.4	83	EXPq-47	−1.9	−24.6
25	EXPS-73	−0.9	−23.4	85	EXPq-51	−1.9	−24.6
27	EXPS-69	−0.9	−23.4	87	EXPq-55	−1.9	−24.6
29	EXPS-65	−0.9	−23.4	89	EXPq-59	−1.9	−24.6
31	EXPS-61	−0.6	−23.4	91	EXPq-63	−1.9	−24.7
33	EXPS-57	−0.6	−23.5	93	EXPq-67	−2.0	−24.7
35	EXPS-53	−0.3	−23.5	95	EXPq-71	−1.9	−24.7
37	EXPS-49	−0.2	−23.4	97	EXPq-75	−1.9	−24.8
39	EXPS-45	−0.2	−23.4	99	EXPq-79	−1.9	−24.7
41	EXPS-41	−0.2	−23.2	101	EXPq-83	−2.0	−24.5
43	EXPS-37	−0.2	−23.2	103	EXPq-87	−2.0	−24.5
45	EXPS-33	−0.2	−23.4	105	EXPq-91	−2.0	−24.3
47	EXPS-29	−0.2	−23.5	107	EXPq-95	−1.9	−24.3
49	EXPS-25	−0.2	−23.7	109	EXPq-99	−1.9	−24.5
51	EXPS-19	−0.2	−24.1	111	EXPq-103	−1.9	−24.5
53	EXPS-15	−0.2	−24.2	113	EXPq-107	−1.9	−24.9
55	EXPS-09	−0.2	−24.2	115	EXPq-111	−1.9	−25.1
57	EXPS-05	−0.2	−24.2	117	EXPq-115	−1.9	−25.2
58	EXPS-01	−0.2	−24.2	119	EXPq-119	−1.9	−25.2